International Journal of Research Studies in Biosciences (IJRSB)
Volume 3, Issue 10, October 2015, PP 66-74
ISSN 2349-0357 (Print) & ISSN 2349-0365 (Online)
www.arcjournals.org

Conformational Analysis of Human Sep15 Mutants to Understand the Role Played from HUB Residues

Stefano Guariniello

Dottorato in Biologia Computazionale, Dipartimento di Biochimica, Biofisica e Patologia generale
Seconda Università degli Studi di Napoli, Napoli, Italy
ste_guar@hotmail.it

Giovanni Colonna

Servizio di Informatica Medica, Azienda Ospedaliera Universitaria
Seconda Università di Napoli, Napoli, Italy
giovanni.colonna@unina2.it

Andrea Polo

Servizio di Informatica Medica, Azienda Ospedaliera Universitaria
Seconda Università di Napoli, Napoli, Italy
a.polo88@libero.it

Giuseppe Castello, Susan Costantini

CROM, Istituto Nazionale Tumori "Fondazione G. Pascale", IRCCS, Napoli, Italy
s.costantini@istitutotumori.na.it, susancostantini77@gmail.com

Abstract: *Human Sep15 (selenoprotein 15KDa) is a selenoprotein altered in different cancers. Recently, it has been demonstrated that Sep15 is up-expressed in cell lines and tissues with hepatocellular carcinoma (HCC). Its three-dimensional structure is composed by a N-terminal region having few regular secondary structure elements and a more structured core with mixed α-helices and β-strands. The residue interaction network analysis on Sep15 model evidenced the presence of three HUB residues, Glu74, Phe154 and Leu159.*

To understand the role of these residues for stabilizing the protein structure, we modeled eight mutants for Sep15 structure. In details, we replaced the three residues with Ala and Gly, and Glu74 and Phe154 with Asp and Trp, respectively, to study the role played from the length and charge of these HUB residues.

Keywords: *Sep15, Mutants, Structure, Molecular dynamics*

1. INTRODUCTION

Some studies have evidenced that the selenium (Se) is able both to block the cellular oxidative damage and to play an important role in cancer development [1]. However this element is incorporated in the selenoproteins as selenocysteine [2]. Recently our group has focused its attention on human Sep15 (selenoprotein 15kDa) [3] that is involved in the quality control of the glycoproteins folding [4] and is highly expressed in organs such as prostate, liver, kidney, testes, and brain [5-6] even if its expression was found altered in lung, breast, colon and prostate cancers [7-8]. In particular, we have demonstrated by RT-qPCR that Sep15 is up-expressed in the two cell lines of hepatocellular carcinoma (HCC), like HepG2 and Huh7, compared to normal hepatocytes [9-10]. This result was also confirmed in thirty HCC tissues of patients, compared to normal liver samples, suggesting the possibility of using this protein as a putative index of endoplasmic reticulum (ER) stress levels in the presence of HCC [10]. Moreover, we modeled the 3D structure of Sep15 to understand the molecular mechanism at the basis of its function [10]. The obtained model showed few regular secondary structure elements at level of the N-terminal region, but a core of α/β structure mixed with some disordered loops. The molecular dynamics simulation evidenced that the structure was enough stable with a highly fluctuating N-terminal region, and, in particular, was stabilized by H-bonds, π-cation interactions, salt bridges and π-stacking interactions and showed three well conserved residues, Glu74, Phe154 and Leu159, which possessed pivotal characteristics to be considered as structural HUB nodes [10].

Since the HUB nodes are important residues in determining the protein structural stability, in this work we modeled the mutants of the human Sep15 to evaluate their role by replacing Glu74, Phe154 and Leu159 with Ala or Gly residues to evaluate the structural effects resulting from the substitution of these amino acids, characterized by very specific side chains, with two residues with very short or absent side chain. Moreover, we modeled also other two mutants by replacing Glu74 and Phe154 with Asp and Trp, respectively, to understand if in Sep 15 the structural role of the negative charge as well as that of the aromatic side chain is dependent on the length of the respective side chains.

2. MATERIALS AND METHODS

2.1. Modeling of Human Sep15 and its Mutants

To model the eight mutants of human Sep15 we used the same procedure reported in an our paper [10]. In details, we performed a comparative modeling strategy using as template the Sep15 structure from Drosophila Melanogaster (PDB: 2A4H) [11] for human region (47-134) and an "ab-initio" method selecting "Intensive" option in Phyre server [12] for the N-terminal region. To select the best models, we used the ProSA program to check the fitness of the sequences relative to the obtained structures and to assign a scoring function [13] and the on-line tool Ramachandran plot 2.0 by dicsoft1 server [14].

All mutant models were subjected to Molecular Dynamics (MD).

2.2. Molecular Dynamics (MD) Simulation and MD Analysis

Molecular Dynamics (MD) simulations of mutants were performed for 20ns at neutral pH and 300K with GROMACS software package (v3.3.1) [15] in agreement with our previous works [10, 16-17]. Each model was inserted in a cubic box filled with SPC216 water molecules using GROMOS43a1 all-atom force field. The systems were subjected to several cycles of energy minimizations and position restraints to equilibrate the protein and the water molecules around the protein. GROMACS routines were used to analyze the trajectories in terms of RMSD, RMSF, H-bonds, secondary structures, gyration radius, energy, cluster and principal components analysis (PCA) [10, 16-17].

Conformations of Sep15 mutants at zero time and after 5, 10, 15 and 20 ns of MD simulation were also studied by construction networks of interacting amino acid pairs (nodes), and focusing on the type of interaction between the different nodes represented as edges in terms of H-bonds, π-cation, π-stacking, salt bridges and interactions with their closest atoms (IAC) as already reported for the wild-type Sep15 [10].

3. RESULTS AND DISCUSSION

3.1. Modelling of Sep15 Mutants

Recently we modeled the three-dimensional structure of the human Sep15 analyzing its structural stability by MD simulations and evaluated the residues that play a key role in structural terms by a residue interaction network (RIN)analysis, identifying three HUB residues, Glu74, Phe154 and Leu159. Since the HUB nodes are important residues in determining the protein structural stability, we modeled the mutants of the human Sep15 to evaluate their importance. The mutants have been named as: Glu74-Ala, Glu74-Gly, Glu74-Asp, Phe154-Ala, Phe154-Gly, Phe154-Trp, Leu159-Ala, and Leu159-Gly. The 3D models of the mutants were built with the same modeling strategy already described in [10]. The analysis of the energetic quality of eight models evidenced that they had a ProSA Z-score ranging by -2.13 to 2.62 that was lower than that obtained for wild-type Sep15 (ProSA Z-score = -2.67) suggesting that even one only mutation is able to induce a little loss of stability. The models of the eight mutants, as well as that of wild-type Sep15 [10], showed few regular elements of secondary structure at level of the N-terminal region, and a core of α/β structure mixed with some disordered loops. They were subjected to MD simulations to evaluate their stability in comparison to the wild-type protein.

3.2. Molecular Dynamics of Sep15 Mutants of Glu74

The MD analysis of Glu74-Ala, Glu74-Gly, and Glu74-Asp mutants compared to the wild-type Sep15 has evidenced that i) Glu74-Ala and wild-type Sep15 had similar trend of RMSD and gyration radius, reaching a relative stability after 6 ns, ii) Glu74-Asp quickly reached the stability after only 3 ns while iii) Glu74-Gly showed an initial instability reaching a stable state after 11 ns and was stabilized from a lesser number of H-bonds (**Figures 1A, B and C**). The RMSF plots showed that the core regions of

all the mutants were quite rigid, while their N-terminal regions (residues 1-55) were highly fluctuating (**Figure 1D**). Moreover, the energy evaluation has evidenced that the Lennard Jones and coulomb potential tended to decrease in all the four MD simulations even if it is evident that Glu74-Gly is the more instable mutant (**Figures 1E and F**), in according to the other analysis **(Figures 1A-D)**.

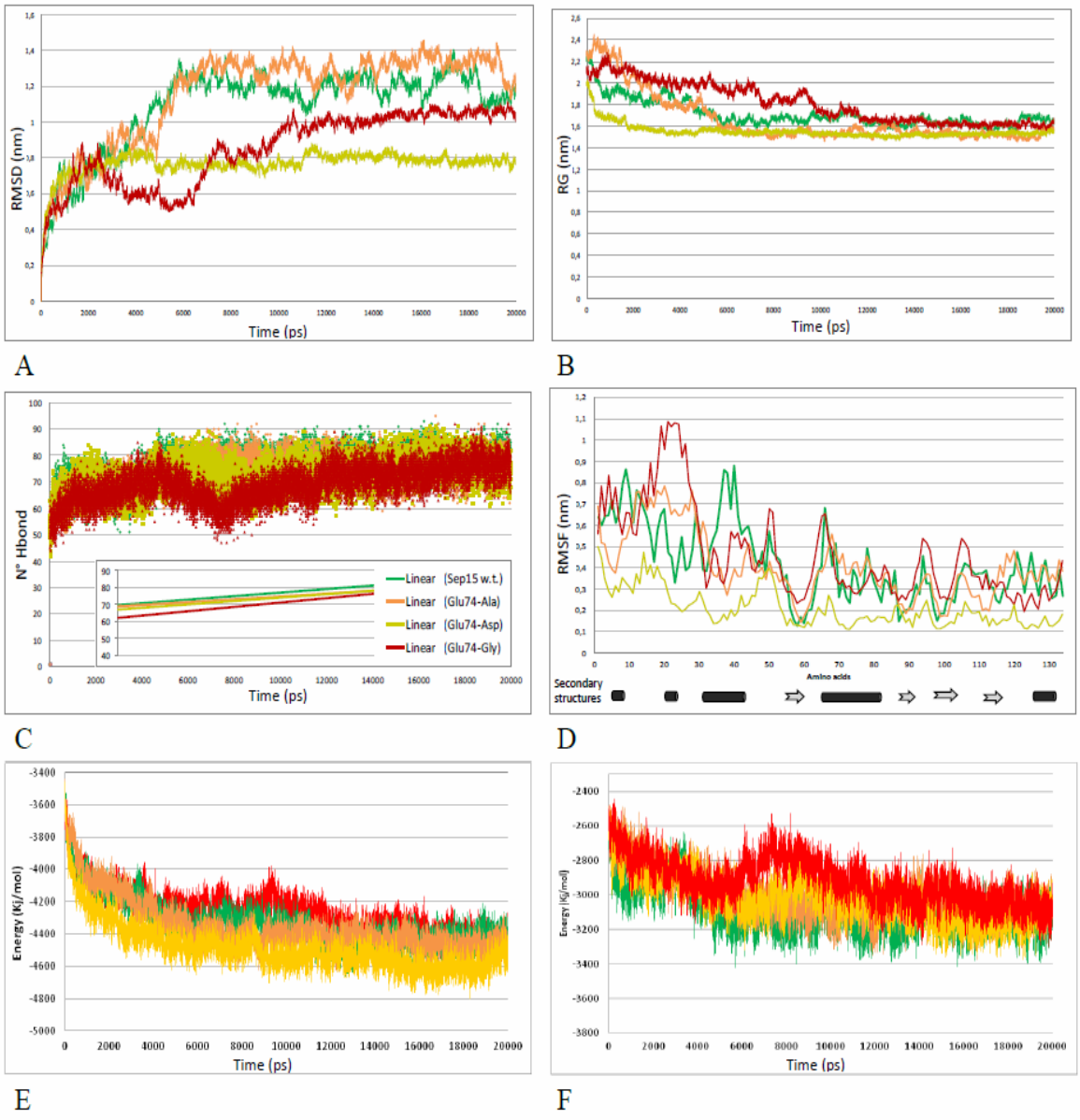

Figure1. *Analysis of MD simulations conducted on Glu74 mutants of Sep15 in terms of: (A) root mean square deviation (RMSD) plot, (B) gyration radius plot, (C) H-bonds plot, (D) root mean square fluctuation (RMSF), (E) Lennard Jones energy and (F) Coulomb energy.*

The evolution of the secondary structure during the MD simulation showed small changes in the N-terminal regions of these mutants (**Figure 2**). In fact, in the wild-type Sep15 the residue Glu74 is positioned at the end of the short third helix in the N-terminal region, but this helix is lacked in the Glu74-Gly model. It is also interesting to note that the helix length decreased in the Glu74-Asp model and increased in the Glu74-Ala model, in good agreement with the relative values for the helical propensity exerted by Asp and Ala. Even the PCA analysis (**Figure 3**) did not show large differences between wild-type Sep15 and its Glu74 mutants except for the mutant Glu74-Asp, which was less moving as already visible in RMSD plot (Figure 1A). Moreover, from the covariance analysis we evidenced that the wild-type Sep15 and the Glu74-Ala had very similar ranges (from -0.378 to 0.783 and from -0.314 to 0.59 respectively) whereas the Glu74-Asp mutant showed a shorter range (from -0.129 to 0.214) (**Figure 4**).

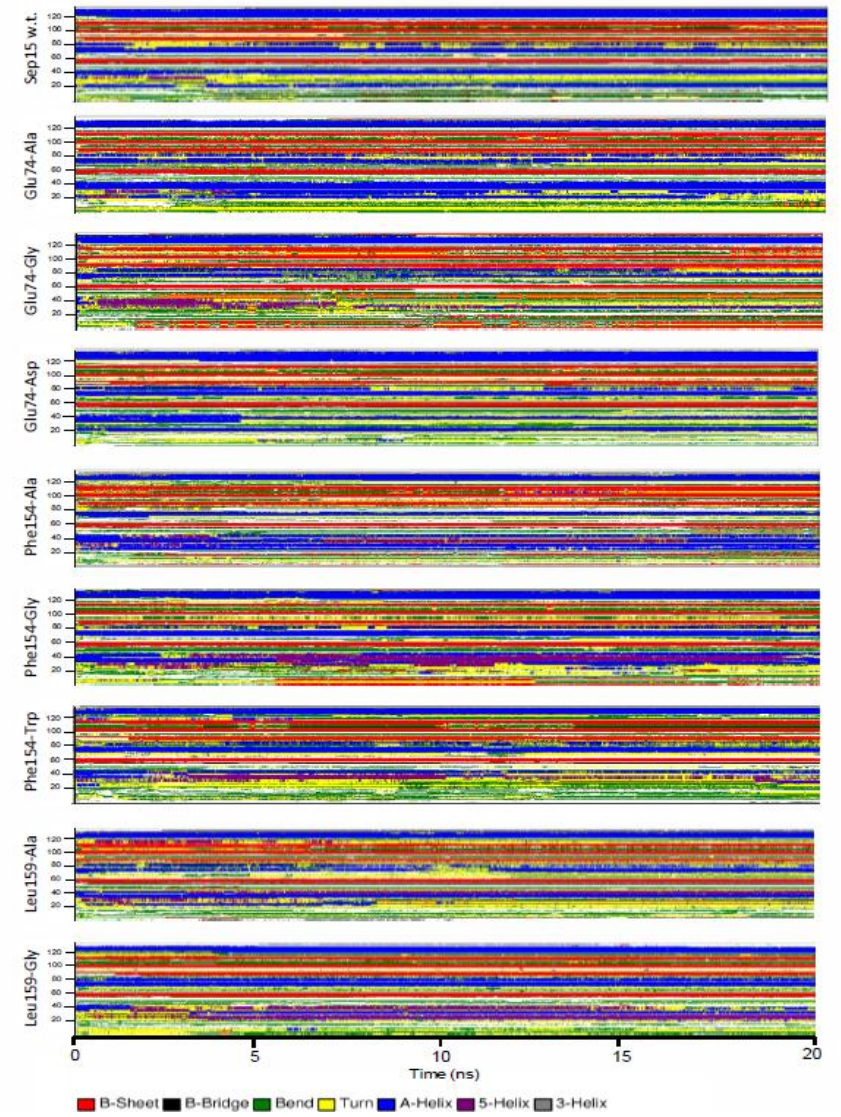

Figure2. *Secondary structure evolution obtained for wild-type Sep15 and the eight mutants during MD simulation.*

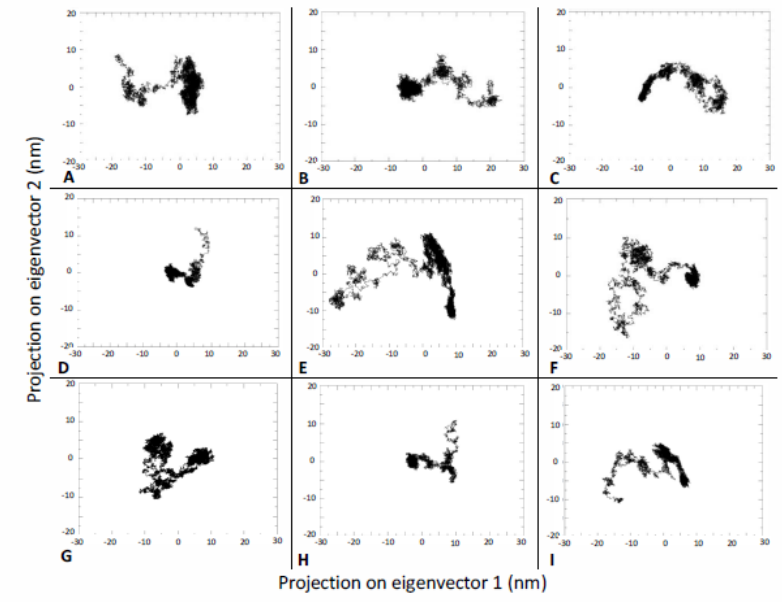

Figure3. *2D projection of simulations onto the plane spanned by the two principal eigenvectors of PCA performed over the C-alpha coordinates for wild-type Sep15 (A), Glu74-Ala (B), Glu74-Gly (C), Glu74-Asp (D), Phe154-Ala (E), Phe154- Gly (F), Phe154-Trp (G), Leu159-Ala (H) and Leu159-Gly (I) mutants.*

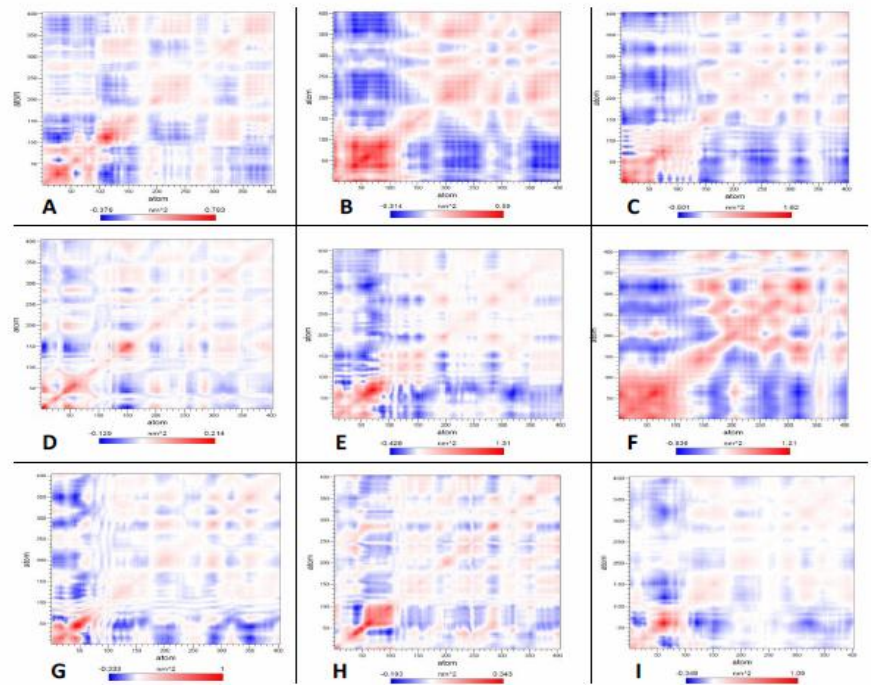

Figure4. *Covariance matrix from PCA analysis obtained during MD simulations for wild-type Sep15 (A), Glu74-Ala (B), Glu74-Gly (C), Glu74-Asp (D), Phe154-Ala (E), Phe154- Gly (F), Phe154-Trp (G), Leu159-Ala (H) and Leu159-Gly (I) mutants.*

Furthermore, the very light red color of the Glu74-Asp mutant suggested a lower amplitude of the fluctuations compared to the other two models of mutants as we can also appreciate by means of the RMSD plots and the PCA. Also, the cluster analysis evidenced that the total number of the clusters was enough similar between the Glu74-Ala mutant and the wild-type Sep15, while it was smaller in the Glu74-Asp mutant and higher in the Glu74-Gly (**Figure 5**). To have more details about the stability of these mutants we evaluated H-bonds, π-cations, π-stackings, IACs, and salt bridges of the three mutants as well as of the wild-type Sep15 after MD simulation. The comparison evidenced that the wild-type protein had the largest number of total H-bonds (92 versus the average number in the mutants of 83). Focusing on residue 74 (**Table 1**), we can see that in all the proteins this residue was always involved in a main chain-main chain (MM) H-bond even if with different residues, such as Gly85 in the wild type Sep15, Cys71 in the Glu74-Ala, Leu159 in the Glu74-Gly and Gly69 in the Glu74-Asp. Moreover the Glu74-Ala and Glu74-Gly mutants showed the smallest number of IACs, probably due to the little extension of the Ala and Gly side chains, reducing their ability to form many contacts with other amino acids (**Table 1**).

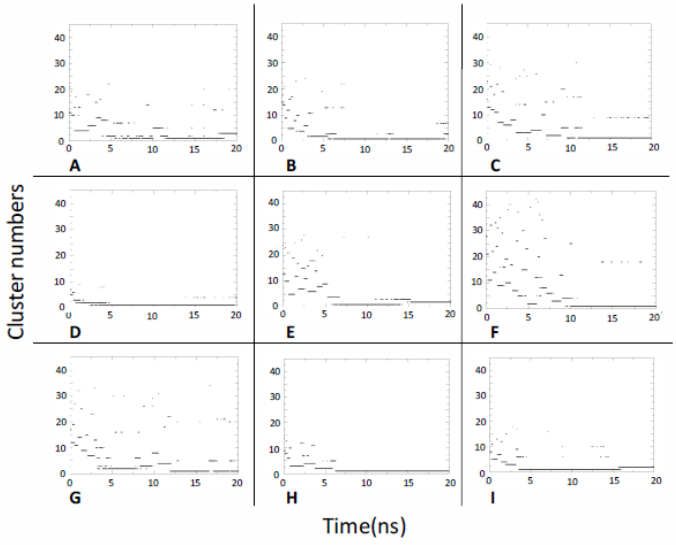

Figure5. *Number of clusters for wild-type Sep15 (A), Glu74-Ala (B), Glu74-Gly (C), Glu74-Asp (D), Phe154-Ala (E), Phe154- Gly (F), Phe154-Trp (G), Leu159-Ala (H) and Leu159-Gly (I) mutants.*

In overall all these data evidenced that i) the presence of Ala in 74 position did not induce evident change in the protein stability compared to Gly and ii) the presence of the negatively charged residues in position 74 did not alter the protein structure suggesting that in this position it is important the negatively charged residue.

3.3. Molecular Dynamics of Sep15 Mutants of Phe154

The MD analysis on the Phe154-Trp, Phe154-Ala and Phe154-Gly mutants compared to the wild-type Sep15 showed that the Phe154-Trp, Phe154-Gly and wild type Sep15 reached a similar stable equilibrated state (with RMSD values of about 1.2 nm) (**Figure 6A**). However, for all the four models the trend of gyration radii decreased while the H-bond number increased suggesting that the four structures became more compact during the simulation (**Figures 6B and C**). Moreover RMSF plots (**Figure 6D**) evidenced that there were differences of conformational fluctuation mainly in the N-terminal region and in the region 100-110, probably due to the absence of IACs between the mutated amino acid 154 and the region 100-102 (as visible in **Table 1**). The energy evaluation has evidenced that the Lennard Jones and coulomb potentials tended to decrease, suggesting the important role of the electrostatic forces (**Figures 6E and F**). The secondary structure evolution (**Figure 2**) showed that i) Phe154-Trp had a shorter length of the last helix, containing the residue 154, perhaps for a sterical bulk due to a greater volume of the Trp side chain, and ii) that the helix containing the residue 74 was shorter and unstable in both Phe154-Trp and Phe154-Ala, while it was lacking in Phe154-Gly. This last result can be explained considering that, due to mutation, the residue 154 has lost some important interactions, such as that with Leu159, with a resulting local destabilization. The PCA (**Figure 3**) showed that Phe154-Ala and Phe154-Gly were more dynamic and conformationally heterogeneous in respect to wild type Sep15 and Phe154-Trp. This result was also confirmed from the covariance analysis which evidenced similar covariance ranges between Sep15 w.t. and Phe154-Trp (from -0.378 to 0.783 and from -0.333 to 1.00, respectively) (**Figure 4**).

Table1. *Interactions between HUB residues with other protein residues. We underline the H-bonds in blue, π-stacking interactions in yellow, and the residues involved in both H-bonds and π-cation interactions in cyan. The residues involved in IAC interactions are reported in black.*

a.a. 74 contact map			
Wild type	Glu74-Ala	Glu74-Asp	Glu74-Gly
		63	
		68	
69		69	
70	70		
71	71	71	
72	72	72	72
76	76	76	76
77	77	77	77
		78	
		79	
	81	81	81
		82	
83			
84			
85			
86			
130			
131			
132			
158			
159			159
		160	160
			161
			162

a.a. 154 contact map			
Wild type	Phe154-Ala	Phe154-Trp	Phe154-Gly
		77	
86		86	
		87	
		88	
128		128	
		129	
130		130	130
		139	
	141	141	
146	146	146	146
		147	
149	149		149
150	150	150	150
151	151	151	151
152	152	152	152
156	156	156	156
157	157	157	157
158	158	158	158
159		159	159

a.a. 159 contact map		
Wild type	Leu159-Ala	Leu159-Gly
		72
		73
74		74
		75
77		
	81	
82	82	
83	83	
84		
85		
86	86	
113	113	113
114	114	
115		
116		
	130	
154	154	
155	155	
156	156	
157	157	157
161		161

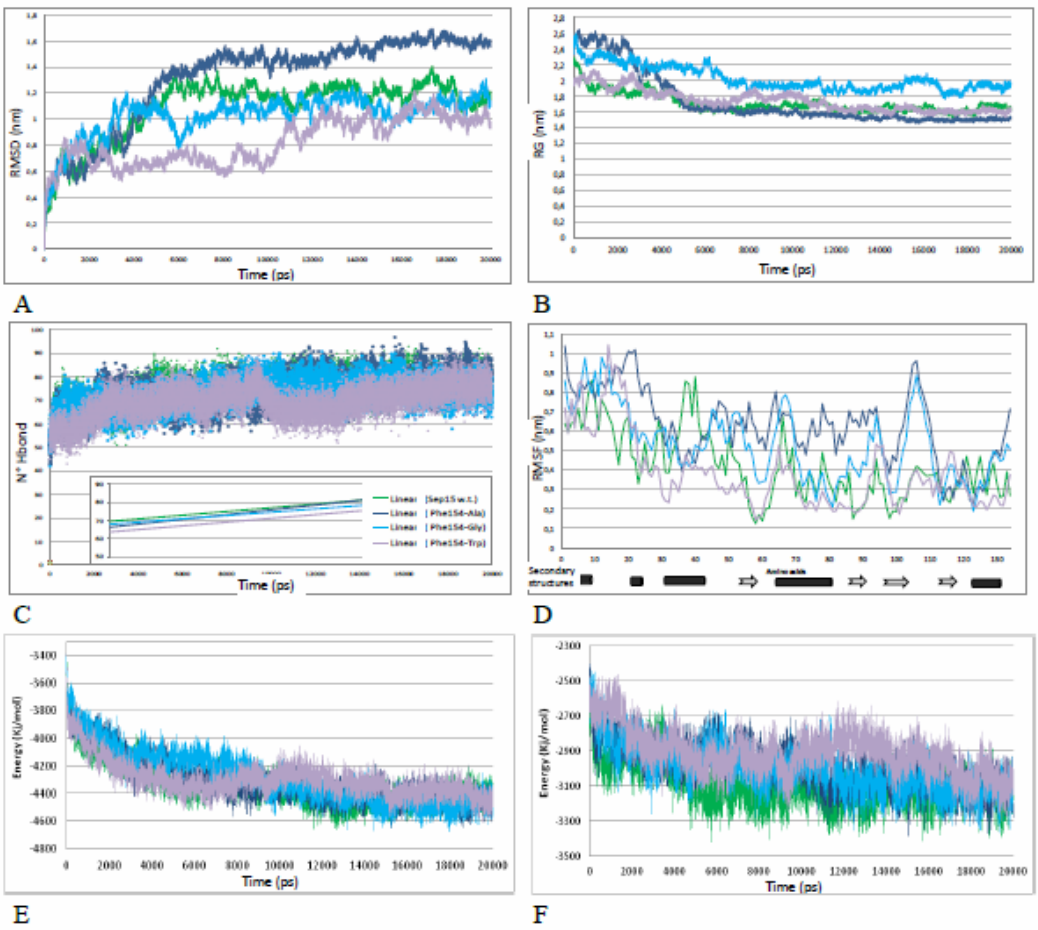

Figure6. *Analysis of MD simulations conducted on Phe154 mutants of Sep15 in terms of: (A) root mean square deviation (RMSD) plot, (B) gyration radius plot, (C) H-bonds plot, (D) root mean square fluctuation (RMSF), (E) Lennard Jones energy and (F) Coulomb energy.*

The understanding of structurally disordered states requires an ensemble interpretation that has been achieved by means of the cluster analysis (**Figure 5**). This analysis showed that wild type Sep15, Phe154-Ala and Phe154-Trp had a comparable number of highly populated clusters whereas Phe154-Gly showing an higher number of clusters during the MD, evidenced that the change of the residue 154 without an appreciable side chain, induced a greater fluctuation, and, hence, a destabilization of the interacting network between the N-terminal region and the core domain.

In conclusion, the change made at the level of the residue 154 produces a loss of interactions and, in particular, of π-cation and π-stacking interactions compared to the wild type protein (**Table 1**) whereas only the Trp154 in the mutant Phe154-Trp showed a great number of IACs, due the greater volume of its side chain (**Table 1**). Relatively to the amino acid 154, its contact maps for the three different mutants showed that this residue interacted through H-bonds with residues 150 and 158 present in the region of closest contacts (149-159).

In overall, the data for the mutants of Phe154 evidenced that i) the presence of Ala or Gly in 154 position resulted to destabilize the core domain of Sep15, and ii) Phe154-Trp had a comparable number of highly populated clusters compared to wild type Sep15 and showed a great number of IACs. Hence, we can highlight the importance of the presence of an aromatic residue in 154 position.

3.4. Molecular Dynamics of Sep15 Mutants for Leu159

MD analysis for Leu159-Ala and Leu159-Gly compared to the wild-type Sep15 showed that all the models reached a stability after 7 ns and a similar compactness in terms of gyration radii and H-bond number (**Figures 7A - C**). The RMSF plots showed that the core remained more rigid in all the mutants and that the N-terminal region was equally mobile in wild-type Sep15 and Leu159-Gly, while appears more static in Leu159-Ala (**Figure 7D**). The energy evaluation has evidenced that the Lennard Jones and coulomb potentials tended to decrease (**Figure 7E-F**). The secondary structure

evolution evidenced that in the two mutants no evident changes were visible at the end of the last helix where is located Leu159, while some changes were located in the helix containing Glu74 found involved in π-helix (**Figure 2**). PCA (**Figure 3**) showed that Leu159-Ala had a smaller movement compared to Leu159-Gly and wild-type Sep15. These observations were also confirmed by the covariance matrices and cluster analysis (**Figures 4 and 5**), which evidenced a more coordinate movement and a smaller number of clusters for Leu159-Ala compared to Leu159-Gly and wild-type Sep15. The total number of H-bonds and IACs in wild-type Sep15 and in the two mutants gave comparable results but a detailed evaluation of Leu-159 showed that: i) it did one H-bond in all the structures, ii) the number of IAC interactions was smaller in the two mutants, and iii) it did not interact both with Glu74 and Phe154 as in the wild type protein but in Leu159-Ala only with Phe154 and in Leu159-Gly only with Glu74 (**Table 1)**. This last observation reasonably explains the instability of the helix containing Glu74.

In overall, the data for the mutants of Leu159 evidenced the importance of Leu in position 159 to maintain the protein structural integrity and the interactions between the N-terminal region and the core domain.

Figure7. *Analysis of MD simulations conducted on Phe154 mutants of Leu159 in terms of: (A) root mean square deviation (RMSD) plot, (B) gyration radius plot, (C) H-bonds plot, (D) root mean square fluctuation (RMSF), (E) Lennard Jones energy and (F) Coulomb energy.*

4. CONCLUSIONS

To confirm the importance of these HUB residues on protein stability, we modeled eight mutants of the human Sep15 replacing Glu74, Phe154 and Leu159 with Ala or Gly residues, and Glu74 and Phe154 with Asp74 and Trp154, respectively, to study the role of charged or aromatic or hydrophobic amino acids in those positions and of their length.

The analyses of the trajectories evidenced that: i) in position 74 it is important the presence of a negatively charged residue, regardless of the length of its side chain length because Asp, with a side chain shorter than Glu, did not alter the protein structure, ii) the mutations in position 154 induced some structural changes both in the last helix and in the helix including the residue 74, and iii) the presence of Leu in position 159 proved important for maintaining the structural integrity of the protein

and the fundamental interactions existing between the N-terminal region and the core domain because its mutation induced the lack of contacts at level of Glu74 or Phe154. Therefore we can conclude that Glu74, Phe154 and Leu159 play a critical role in the structural stability of the human Sep15.

REFERENCES

[1] Valko M., Rhodes C. J., Moncol J., Izakovic M., Mazur M., Free radicals, metals and antioxidants in oxidative stress-induced cancer, Chemico-Biological Interactions 160, 1–40 (2006).

[2] Bellinger F. P., Raman A. V., Reeves M. A., Berry M.J., Regulation and function of selenoproteins in human disease, Biochemical Journal 422, 11–22 (2009).

[3] Guariniello S., Colonna G., Guerriero E., Capone F., Costantini M., Di Bernardo G., Accardo M., Castello G., Costantini S., Sequence and Structure Analysis of Human Selenoprotein 15kDa (Sep15), an Up-Expressed Protein in the Hepatocellular Carcinoma, International Journal of Research Studies in Biosciences 3, 1-14 (2015).

[4] Korotkov K. V., Kumaraswamy E., Zhou Y., Hatfield D. L., Gladyshev V. N., Association between the 15-kDa Selenoprotein and UDP-glucose: Glycoprotein Glucosyltransferase in the Endoplasmic Reticulum of Mammalian Cells, The Journal of Biological Chemistry 276, 15330–15336 (2001).

[5] Labunskyy V. M., Yoo M. H., Hatfield D. L., Gladyshev V. N., Sep15, a Thioredoxin-like Selenoprotein, Is Involved in the Unfolded Protein Response and Differentially Regulated by Adaptive and Acute ER Stresses, Biochemistry 48, 8458-8465 (2009).

[6] Kasaikina M. V., Fomenko D. E., Labunskyy V. M., Lachke1 S. A., Qiu W., Moncaster J. A., Zhang J., Wojnarowicz Jr M. W., Natarajan S. K., Malinouski M., Schweizer U., Tsuji P. A., Carlson B. A., Maas R. L., Lou M. F., Goldstein L. E., Hatfield D. L., Gladyshev V. N., 15 kDa selenoprotein (Sep15) knockout mice: roles of Sep15 in redox homeostasis and cataract development, Journal of Biological Chemistry M111, 259218 (2011).

[7] Kumaraswamy E., Korotkov K. V., Diamond A. M., Gladyshev V. N., Hatfield D. L., Genetic and functional analysis of mammalian Sep15 selenoprotein, Methods in Enzymology 347, 187-197 (2002).

[8] Tsuji P. A., Naranjo-Suarez S., Carlson B. A., Tobe R., Yoo M. H., Davis C. D., Deficiency in the 15 kDa selenoprotein inhibits human colon cancer cell growth, Nutrients 3, 805–817 (2011)

[9] Guariniello S., Di Bernardo G., Colonna G., Cammarota M., Castello G., Costantini S., Evaluation of the selenotranscriptome expression in two hepatocellular carcinoma cell lines, Analitical Cell Pathology 2015, 419561 (2015).

[10] Guariniello S., Colonna G., Guerriero E., Capone F., Costantini M., Di Bernardo G., Accardo M., Castello G., Costantini S., Sequence and Structure Analysis of Human Selenoprotein 15kDa (Sep15), an Up-Expressed Protein in the Hepatocellular Carcinoma, International Journal of Research Studies in Biosciences (IJRSB) 3, 112-125 (2015).

[11] Ferguson A.D., Labunskyy V.M., Fomenko D.E., Arac D., Chelliah Y., Amezcua C.A., Rizo J., Gladyshev V.N., Deisenhofer J., NMR structures of the selenoproteins Sep15 and SelM reveal redox activity of a new thioredoxin-like family, The Journal of Biological Chemistry 281, 3536–3543 (2006).

[12] Kelley L. A., Mezulis S., Yates C. M., Wass M. N., Sternberg M. J., The Phyre2 web portal for protein modeling, prediction and analysis, Nature Protocol 10, 845-58 (2015).

[13] Sippl M.J., Recognition of errors in three-dimensional structures of proteins, Proteins 17, 355–362 (1993).

[14] Gopalakrishnan K., Sowmiya G., Sheik S.S., Sekar K., Ramachandran plot on the web (2.0), Protein and Peptide Letters 14, 669–671 (2007).

[15] Van Der Spoel D., Lindahl E., Hess B., Groenhof G., Mark A.E., Berendsen H.J., GROMACS: fast, flexible, and free, Journal of Computational Chemistry 26, 1701–1718 (2005).

[16] Guariniello S., Colonna G., Raucci R., Costantini M., Di Bernardo G., Bergantino F., Castello G., Costantini S., Structure–function relationship and evolutionary history of the human selenoprotein M (SelM) found over-expressed in hepatocellular carcinoma, Biochimica et Biophysica Acta 1844, 447–456 (2014).

[17] Raucci R., Colonna G., Giovane A., Castello G., Costantini S., N-terminal region of human chemokine receptor CXCR3: Structural analysis of CXCR3(1–48) by experimental and computational studies, Biochimica et Biophysica Acta (BBA) - Proteins and Proteomics 1884, 1868-1880 (2014).